# Large area, freestanding GaN nanocolumn membrane with bottom subwavelength nanostructure

**Yongjin Wang\*, Fangren Hu, Yoshiaki Kanamori, Tong Wu, Kazuhiro Hane**

*Department of nanomechanics, Tohoku University, Sendai 980-8579, Japan*
*\*wang@hane.mech.tohoku.ac.jp*

**Abstract:** We propose, fabricate and characterize the freestanding GaN nanocolumn membrane with bottom subwavelength nanostructures. The GaN nanocolumns are epitaxially grown on freestanding nanostructured silicon substrate that is achieved by a combination of self-assemble technique and silicon-on-insulator (SOI) technology. Optical reflection is greatly suppressed in the visible range due to the graded refractive index effect of subwavelength nanostructures. The freestanding GaN nanocolumn membrane is realized by removing silicon substrate from the backside, eliminating the silicon absorption of the emitted light and leading to a strong blue emission from the bottom side. The obtained structures also demonstrate the potential application for anti-reflective (AR) coating and GaN-Si hybrid microelectromechanical system (MEMS).

---

## References and links

1. F. A. Ponce, and D. P. Bour, "Nitride-based semiconductors for blue and green light-emitting devices," Nature **386**(6623), 351–359 (1997).
2. A. C. Tamboli, E. D. Haberer, R. Sharma, K. H. Lee, S. Nakamura, and E. L. Hu, "Room-temperature continuous-wave lasing in GaN/InGaN microdisks," Nat. Photonics **1**(1), 61–64 (2007).
3. M. R. Krames, O. B. Shchekin, R. Mueller-Mach, G. O. Mueller, L. Zhou, G. Harbers, and M. G. Craford, "Status and Future of High-Power Light-Emitting Diodes for Solid-State Lighting," J. Display Technol. **3**(2), 160–175 (2007).
4. H. Yoshida, Y. Yamashita, M. Kuwabara, and H. Kan, "A 342-nm ultraviolet AlGaN multiple-quantum-well laser diode," Nat. Photonics **2**(9), 551–554 (2008).
5. J. J. Wierer, A. David, and M. M. Megens, "III-nitride photonic-crystal light-emitting diodes with high extraction efficiency," Nat. Photonics **3**(3), 163–169 (2009).
6. H. M. Kim, Y. H. Cho, H. Lee, S. I. Kim, S. R. Ryu, D. Y. Kim, T. W. Kang, and K. S. Chung, "High-Brightness light emitting diodes using dislocation-free indium gallium nitride/gallium nitride multiquantum-well nanorod arrays," Nano Lett. **4**(6), 1059–1062 (2004).
7. Y. J. Lee, S. Y. Lin, C. H. Chiu, T. C. Lu, H. C. Kuo, S. C. Wang, S. Chhajed, J. K. Kim, and E. F. Schubert, "High output power density from GaN-based two-dimensional nanorod light-emitting diode arrays," Appl. Phys. Lett. **94**(14), 141111 (2009).
8. S. M. Kim, T. Y. Park, S. J. Park, S. J. Lee, J. H. Baek, Y. C. Park, and G. Y. Jung, "Nanopatterned aluminum nitride template for high efficiency light-emitting diodes," Opt. Express **17**(17), 14791–14799 (2009).
9. S. W. Ryu, J. Park, J. K. Oh, D. H. Long, K. W. Kwon, Y. H. Kim, J. K. Lee, and J. H. Kim, "Analysis of improved efficiency of InGaN light-emitting diode with bottom photonic crystal fabricated by anodized aluminum oxide," Adv. Funct. Mater. **19**(10), 1650–1655 (2009).
10. F. Schulze, A. Dadgar, J. Bläsing, A. Diez, and A. Krost, "Metalorganic vapor phase epitaxy grown InGaN/GaN light-emitting diodes on Si(001) substrate," Appl. Phys. Lett. **88**(12), 121114 (2006).
11. H. W. Choi, K. N. Hui, P. T. Lai, P. Chen, X. H. Zhang, S. Tripathy, J. H. Teng, and S. J. Chua, "Lasing in GaN microdisks pivoted on Si," Appl. Phys. Lett. **89**(21), 211101 (2006).
12. S. Tripathy, V. K. X. Lin, S. L. Teo, A. Dadgar, A. Diez, J. Bläsing, and A. Krost, "InGaN/GaN light emitting diodes on nanoscale silicon on insulator," Appl. Phys. Lett. **91**(23), 231109 (2007).
13. T. Zimmermann, M. Neuburger, P. Benkart, F. J. Hernández-Guillén, C. Pietzka, M. Kunze, I. Daumiller, A. Dadgar, A. Krost, and E. Kohn, "Piezoelectric GaN Sensor Structures," IEEE Electron Device Lett. **27**(5), 309–312 (2006).
14. Z. Yang, R. N. Wang, S. Jia, D. Wang, B. S. Zhang, K. M. Lau, and K. J. Chen, "Mechanical characterization of suspended GaN microstructures fabricated by GaN-on-patterned-silicon technique," Appl. Phys. Lett. **88**(4), 041913 (2006).

15. Y. B. Tang, Z. H. Chen, H. S. Song, C. S. Lee, H. T. Cong, H. M. Cheng, W. J. Zhang, I. Bello, and S. T. Lee, "Vertically aligned p-type single-crystalline GaN nanorod arrays on n-type Si for heterojunction photovoltaic cells," Nano Lett. **8**(12), 4191–4195 (2008).
16. R. Calarco, R. J. Meijers, R. K. Debnath, T. Stoica, E. Sutter, and H. Lüth, "Nucleation and growth of GaN nanowires on Si(111) performed by molecular beam epitaxy," Nano Lett. **7**(8), 2248–2251 (2007).
17. S. D. Hersee, X. Y. Sun, and X. Wang, "The controlled growth of GaN nanowires," Nano Lett. **6**(8), 1808–1811 (2006).
18. F. R. Hu, Y. Kanamori, K. Ochi, Y. Zhao, M. Wakui, and K. Hane, "A 100 nm thick InGaN/GaN multiple quantum-well column-crystallized thin film deposited on Si(111) substrate and its micromachining," Nanotechnology **19**(3), 035305 (2008).
19. A. Kikuchi, M. Kawai, M. Tada, and K. Kishino, "InGaN/GaN Multiple Quantum Disk Nanocolumn Light-Emitting Diodes Grown on (111) Si Substrate," Jpn. J. Appl. Phys. **43**(No. 12A), L1524–L1526 (2004).
20. H. Sekiguchi, K. Kishino, and A. Kikuchi, "GaN/AlGaN nanocolumn ultraviolet light-emitting diodes grown on n-(111) Si by RF-plasma-assisted molecular beam epitaxy," Electron. Lett. **44**(2), 151–152 (2008).
21. H. Sameshima, M. Wakui, F. R. Hu, and K. Hane, "A freestanding GaN/HfO$_2$ membrane grown by molecular beam epitaxy for GaN-Si hybrid MEMS," IEEE J. Sel. Top. Quantum Electron. **15**(5), 1332–1337 (2009).
22. T. Ono, N. Orimoto, S. S. Lee, T. Simizu, and M. Esashi, "RF-plasma-assisted fast atom beam etching," Jpn. J. Appl. Phys. **39**(Part 1, No. 12B), 6976–6979 (2000).
23. J. Zhu, Z. F. Yu, G. F. Burkhard, C. M. Hsu, S. T. Connor, Y. Q. Xu, Q. Wang, M. McGehee, S. H. Fan, and Y. Cui, "Optical absorption enhancement in amorphous silicon nanowire and nanocone arrays," Nano Lett. **9**(1), 279–282 (2009).
24. C. M. Hsu, S. T. Connor, M. X. Tang, and Y. Cui, "Wafer-scale silicon nanopillars and nanocones by Langmuir–Blodgett assembly and etching," Appl. Phys. Lett. **93**(13), 133109 (2008).
25. S. Chhajed, M. F. Schubert, J. K. Kim, and E. F. Schubert, "Nanostructured multilayer graded-index antireflection coating for Si solar cells with broadband and omnidirectional characteristics," Appl. Phys. Lett. **93**(25), 251108 (2008).
26. W. L. Min, B. Jiang, and P. Jiang, "Bioinspired self-cleaning antireflection coatings," Adv. Mater. **20**(20), 3914–3918 (2008).
27. H. B. Xu, N. Lu, D. P. Qi, J. Y. Hao, L. G. Gao, B. Zhang, and L. F. Chi, "Biomimetic antireflective Si nanopillar arrays," Small **4**(11), 1972–1975 (2008).
28. Y. J. Wang, F. R. Hu, Y. Kanamori, T. Wu, and K Hane, "Over 200-fold enhancement of light extraction from freestanding GaN nanocolumn slab with bottom subwavelength," to be submitted.
29. C. H. Chiu, P. C. Yu, H. C. Kuo, C. C. Chen, T. C. Lu, S. C. Wang, S. H. Hsu, Y. J. Cheng, and Y. C. Chang, "Broadband and omnidirectional antireflection employing disordered GaN nanopillars," Opt. Express **16**(12), 8748–8754 (2008).
30. S. L. Diedenhofen, G. Vecchi, R. E. Algra, A. Hartsuiker, O. L. Muskens, G. Immink, E. P. A. M. Bakkers, W. L. Vos, and J. G. Rivas, "Broad-band and Omnidirectional Antireflection Coatings Based on Semiconductor Nanorods," Adv. Mater. **21**(9), 973–978 (2009).
31. C. H. Chang, Yu. Peichen, and C. S. Yang, "Broadband and omnidirectional antireflection from conductive indium-tin-oxide nanocolumns prepared by glancing-angle deposition with nitrogen," Appl. Phys. Lett. **94**(5), 051114 (2009).
32. H. Y. Chen, H. W. Lin, C. Y. Wu, W. C. Chen, J. S. Chen, and S. Gwo, "Gallium nitride nanorod arrays as low-refractive-index transparent media in the entire visible spectral region," Opt. Express **16**(11), 8106–8116 (2008).
33. K. Kusakabe, A. Kikuchi, and K. Kishino, "Characterization of overgrown GaN layers on nano-columns grown by RF-molecular beam epitaxy," Jpn. J. Appl. Phys. **40**(Part 2, No. 3A), L192–L194 (2001).
34. C. H. Chiu, H. H. Yen, C. L. Chao, Z. Y. Li, Y. Peichen, H. C. Kuo, T. C. Lu, S. C. Wang, K. M. Lau, and S. J. Cheng, "Nanoscale epitaxial lateral overgrowth of GaN-based light-emitting diodes on a SiO$_2$ nanorod-array patterned sapphire template," Appl. Phys. Lett. **93**(8), 081108 (2008).

## 1. Introduction

GaN-based materials are of great interest for their light emission application because the emission wavelength can cover over a broad range by tuning the indium or aluminum content [1–5]. The overall efficiency of GaN light emitting diodes (LEDs) is determined by the internal quantum efficiency and the light extraction efficiency. Chung *et al.* overcame the challenge of the realization of current-junction nanodevices and demonstrated high brightness GaN LEDs using the GaN nanorod arrays due to their high quantum efficiency [6]. Lee *et al.* also presented the GaN LEDs with two-dimensional nanorod arrays on sapphire substrate [7]. In order to improve the light extraction efficiency, Jung *et al.* introduced the GaN LEDs grown on nanopatterned AlN template [8]. They revealed the notable increase of the bottom side emission due to the graded refractive index effect of the nanopatterned AlN. Kim *et al.* also reported the GaN LEDs with bottom photonic crystal where sapphire is substrate of choice [9]. However, sapphire substrate is still expensive for general lighting application and difficult to manufacture.

Recently, the fabrication of GaN-on-silicon light emission devices and the hybrid integration of GaN light source with silicon microelectromechnical system (MEMS) have been made possible due to the advances in the deposition of GaN-based films on silicon substrate and the mature silicon manufacturing [10–14]. The GaN nanocolumns can be epitaxially grown on silicon substrate [15–18], and Kikuchi *et al.* realized the GaN nanocolumn LEDs on silicon substrate [19,20]. Sameshima *et al.* presented a freestanding GaN/HfO$_2$ membrane for GaN-Si hybrid MEMS [21]. It's promising to maintain motivation to conduct fundamental studies as well as applied research on novel GaN-based devices using GaN-on-silicon system.

Here, we propose and experimentally realize a freestanding GaN nanocolumn membrane with bottom subwavelength nanostructures. The GaN nanocolumns are epitaxially grown on freestanding nanostructured silicon substrate by a combination of self-assemble technique and silicon-on-insulator (SOI) technology. The silicon substrate is subsequently removed to generate the freestanding GaN nanocolumn membrane, eliminating silicon absorption and leading to a strong blue emission from the bottom side. The obtained structures also demonstrate the promising application for anti-reflective (AR) coating in the visible range and GaN-Si hybrid MEMS.
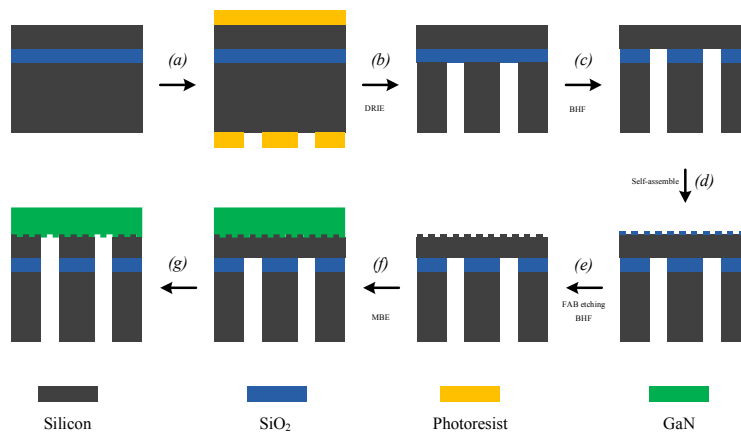
## 2. Device fabrication



Fig. 1. Schematic fabrication process of the freestanding GaN nanocolumn membrane with bottom subwavelength nanostructures.

Figure 1 schematically illustrates the fabrication process of the freestanding GaN nanocolumn membrane with bottom subwavelength nanostructures. The starting 2cm × 2cm n-type (100) SOI substrate consists of 10μm silicon top layer, 1μm buried oxide layer and 200μm silicon substrate. The silicon substrate was first patterned from the backside by photolithography (*steps a*). The silicon substrate was then etched down to the buried oxide layer using deep reactive ion etching (D-RIE), where the buried oxide layer acted as an etching stop layer (*steps b*). After removing the residual photoresist, the buried oxide layer was removed by buffered hydrofluoric acid (BHF) etching (*steps c*). Subsequently, 170nm-diameter silica nanospheres were spin-coated onto the silicon top surface, which made silica nanospheres self-assemble into a close-packed monolayer. The prepared template was then kept in an oven at 90°C for 10min and 145°C for 30min, respectively, evaporating the solvent (*steps d*). The subwavelength nanostructure patterns were transferred into the silicon top layer by fast atom beam (FAB) etching where silica nanospheres served as an etching mask. FAB etching was conducted with the SF$_6$ flow of 5.6sccm at the high voltage of 2.0KV and the accelerated current of 20mA. The residual silica particles were removed by BHF etching to generate subwavelength nanostructures on the silicon top layer (*steps e*). The InGaN/GaN multiple quantum wells (MQWs) active layers were deposited on the prepared SOI template by molecular beam epitaxy (MBE) with radio frequency nitrogen plasma as gas source. The

resultant GaN nanocolumn structure incorporated 200nm low-temperature buffer-layer, 300nm high-temperature GaN layer, six pair 3nm InGaN/9nm GaN MQWs layer and 10nm GaN top-layer (*steps f*). Finally, the freestanding silicon membrane was removed by RIE of silicon from the backside, which made the GaN nanocolumn membrane totally suspend in space (*steps g*).

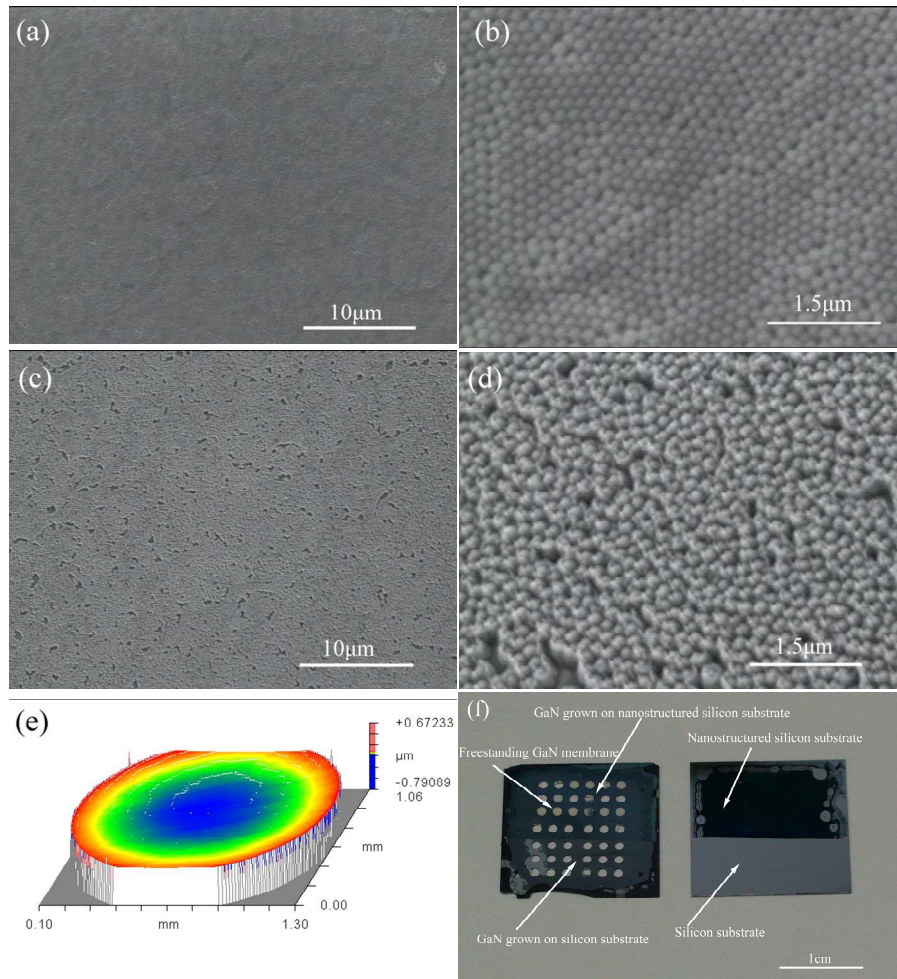## 3. Experimental results and discussion



Fig. 2. (a) and (b) the 30°tilt-view SEM images of the close-packed monolayer of silica nanospheres; (c) and (d) the tilt-view SEM images of fabricated subwavelength silicon nanostructure; (e) three-dimensional surface profile of freestanding silicon slab; (f) photograph of silicon substrate and the freestanding GaN nanocolumn membrane.

Figures 2(a) and 2(b) show the 30°tilt-view scanning electron microscope (SEM) images of silica nanospheres that form a close-packed monolayer on the silicon top layer and display short-range order. In association with FAB etching, subwavelength nanostructures are transferred into the silicon top layer, as illustrated in Figs. 2(c) and 2(d). FAB etching is a neutral dry etching technique and has good directionality [22]. Hence, silica nanospheres are etched and the lateral dimensions of silica nanospheres shrink during FAB etching. The fabricated subwavelength silicon nanostructures are thus gradually tapered. The depths of the resultant silicon nanostructures are about 170nm which can be controlled by FAB etching time. The residual silica particles can be removed by subsequent BHF etching. Figure 2(e) illustrates the three-dimensional surface profiles of the freestanding silicon membrane

measured by an optical interferometer. The surface deflection from the silicon substrate side is slightly downward due to the residual stress, and the peak-to-valley (PV) value is measured at ~0.299μm for 1200μm-diameter silicon membrane. Figure 2(f) shows the photograph of two resultant samples for comparison. The right sample is the silicon substrate with subwavelength nanostructures. In order to eliminate the variation in device properties from wafer to wafer, the sample is partially protected during FAB etching, and subwavelength silicon nanostructures are well realized in the large device area. The left sample is the freestanding GaN nanocolumn membrane with bottom subwavelength nanostructure, where the silicon substrate is removed by RIE from the backside. 31 out of 42 samples are successfully achieved now, and the yield can be further improved by optimizing RIE of silicon from the backside that is the core process for fabricating the freestanding GaN nanocolumn membrane with large area.
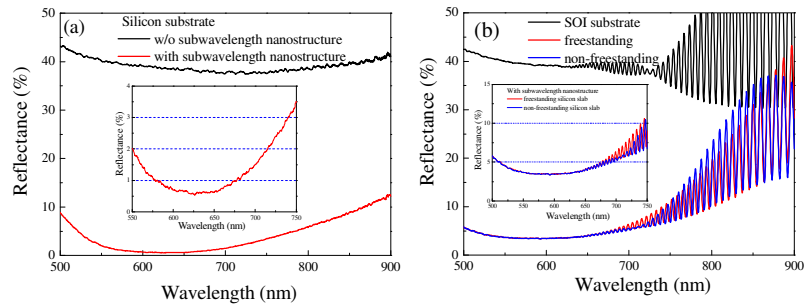


Fig. 3. (a) Measured reflectivity of subwavelength silicon nanostructures on silicon substrate; (b) measured reflectivity of subwavelength silicon nanostructures on SOI substrate.

Subwavelength silicon nanostructures that are the tapered column profiles can function as AR coating in the visible range due to the graded refractive index effect [23–27]. As shown in the inset of Fig. 3(a), the reflectivity is significantly reduced in the visible range. Especially, the reflectivity is below ~1% over the range of 578-678nm. The rotation speed during the spin-coating step of silica nanospheres and FAB etching time are the two core parameters to control the fabricated subwavelength silicon nanostructures which will be discussed elsewhere [28]. Although the freestanding silicon membrane has a slight deflection, subwavelength nanostructures are well obtained in the prepared SOI template. In the visible range, the reflectivity is also greatly reduced by the graded refractive index effect of the subwavelength nanostructures, as illustrated in Fig. 3(b). The interference fringes for SOI substrate are attributed to the multiple reflections of visible light at the silicon/air and the silion/the buried oxide interfaces, and the interference fringes for the freestanding silicon membrane is caused by the multiple reflections at the silicon/air interfaces. These results experimentally demonstrate that subwavelength silicon nanostructure can effectively serve as graded index AR coating in the visible range.

Figure 4(a) shows SEM image of the freestanding GaN slab obtained from the silicon substrate side. The diameter of the freestanding GaN nanocolumn membrane is 1200μm. The silicon substrate is etched from the backside to make the GaN nanocolumn membrane totally suspend in space. Figures 4(b) and 4(c) show the 30°tilt-view SEM images of the freestanding GaN nanocolum membrane from the top side. The freestanding GaN nanocolumns are well achieved, and their diameters are less than 100nm. The bottom surfaces of the freestanding GaN nanocolumn membrane are characterized in Figs. 4(d)-(f). Regarding the GaN nanocolumns grown on nanostructured silicon substrate, subwavelength GaN nanostructures are clearly observed as shown in Figs. 4(d) and 4(e). It can be attributed to (1) nanostructured silicon template and (2) surface modification caused by RIE of silicon. Figure 4(f) illustrates the bottom GaN surface where the GaN nanocolumns are grown on the flat silicon substrate. The surface is slightly roughened which is caused by the surface modification during RIE of silicon.
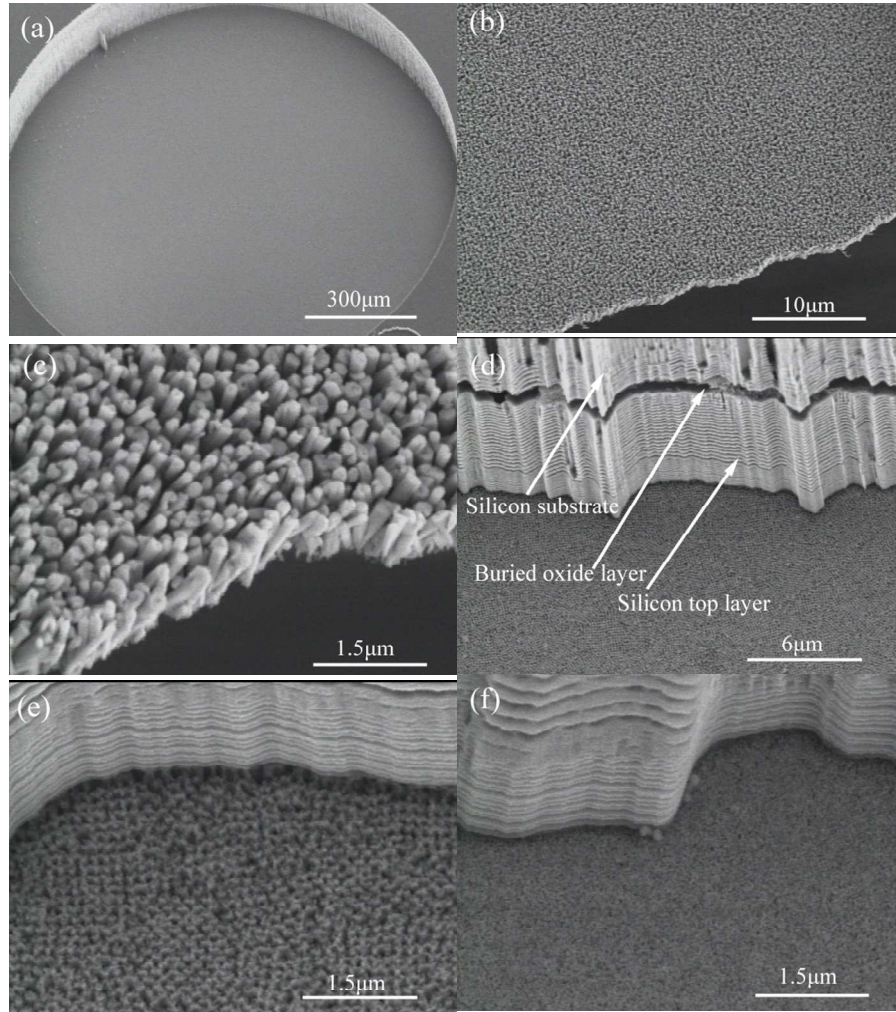
Fig. 4. (a) Sample of the freestanding GaN nanocolumn membrane obtained from silicon substrate side; (b) and (c) the 30°tilt-view SEM images of the freestanding GaN nanocolumns obtained from the top side; (d) and (e) the tilt-view SEM images of the bottom surface of the subwavelength GaN nanostructures; (f) the bottom surface of the GaN nanocolumns grown on the flat silicon substrate.

The semiconductor nanocolumns can also suppress optical reflection over a broad wavelength range [29–31]. Figure 5(a) shows the measured reflectivity of the GaN nanocolumn slab where the flat silicon substrate is kept. Compared with that of Fig. 3(b), the reflectivity is greatly reduced due to the introduction of the GaN nanocolumns, revealing that the GaN nanocolumns can effectively serve as AR coating to decrease optical reflection. However, the refractive index changes immediately at the GaN/flat silicon interface, leading to the reflection of light. Hence, the interference fringes are clearly observed in the reflectance spectra which come from the multiple reflections at the different medium interferences [32]. Figure 5(b) illustrates the measured reflectivity of the GaN nanocolumn slab where the silicon substrate is subwavelength nanostructured and originated from that of Fig. 3(b). In this case, subwavelength nanostructures provide a graded refractive index step at the GaN/nanostructured silicon interface, hence, the reflection is reduced over a broad wavelength range and the interference characteristics are also suppressed. Especially, the reflectivity is below ~2% over the wavelength range of 500-750nm.
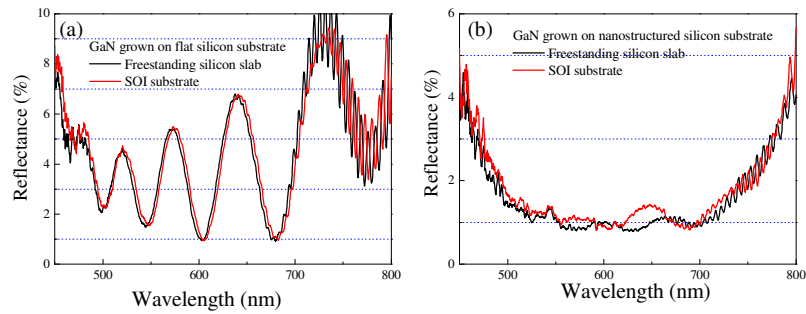
Fig. 5. (a) Measured reflectivity of the GaN nanocolumn slab grown on the flat silicon substrate; (b) measured reflectivity of the GaN nanocolumn slab grown on nanostructured silicon substrate.

The photoluminescence (PL) measurements are performed at room temperature using a 325nm He-Cd laser source. The pump laser beam is focused onto the GaN slab through a UV-compatible objective lens (numerical aperture: 0.36), and the emitted light is collected by the same objective lens and measured using a multichannel Hamamatsu analyzer system. Figure 6(a) shows the PL spectra of the GaN nanocolumn slabs grown on the flat silicon substrate. Regarding the non-freestanding GaN slab, the PL peaks at ~365nm and ~520nm are attributed to the excitation of the top GaN crystal and the InGaN/GaN MQWs active layers, respectively. A clear enhancement in PL intensity is observed because silicon absorption of the emitted light is eliminated for the freestanding GaN nanocolumn slab, and the broad PL peak for the excitation of the InGaN/GaN MQWs is measured at ~526nm. The emission peak of the GaN crystal disappears when the laser beam is pumped onto the freestanding GaN nanocolumn slab from the bottom surface. Compared with the capping GaN layer, the buffer layer that is necessary for the growth of GaN nanocolumns has lower effective refractive index. Hence, more light can escape in air from the bottom side. The GaN nanocolumns produce a strong blue emission peak at ~471nm with a full-width at half-maximum (FWHM) of about 75nm, which is associated with the InGaN/GaN MQWs. The enhancements of the integrated intensity and the peak intensity that are normalized to those of the non-freestanding GaN nanocolumn slab are about 1.6 times and 3 times, respectively. As to the GaN nanocolumn slab grown on nanostructured silicon substrate, the emission peak of the top GaN crystal is almost the same, while a blue shift is observed for the excitation of the InGaN/GaN MQWs, as shown in Fig. 6(b). The blue shift can be attributed to the occurrence of strain relaxation by growing GaN nanocolumns on nanostructured silicon substrate [33,34]. The broad PL peaks are measured at ~466nm for the non-freestanding GaN slab and ~482nm for the freestanding GaN slab, respectively. A 10.8-fold enhancement in PL peak intensity is measured from the bottom side. The emission peak of the InGaN/GaN MQWs is observed at ~437nm with a FWHM of about 81nm, and the enhancement of the integrated intensity is increased by about 5.1 times.
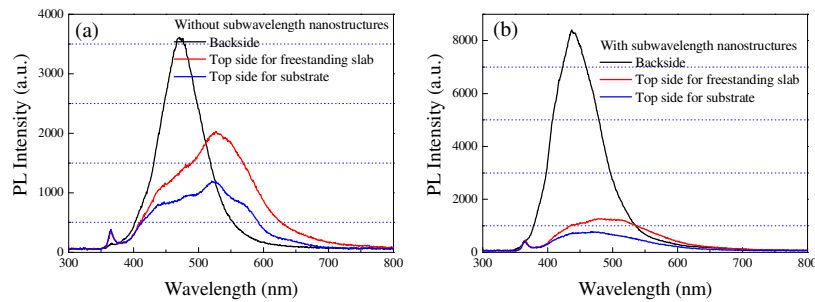
Fig. 6. (a) The PL spectra of the GaN nanocolumn slab grown on the flat silicon substrate; (b) the PL spectra of the GaN nanocolumn slab grown on nanostructured silicon substrate.

## 4. Conclusions

In conclusion, the freestanding GaN nanocolumn membrane with bottom subwavelength nanostructures is successfully realized by a combination of self-assemble technique, FAB etching, silicon processing and MBE growth. Some interesting results are experimentally demonstrated: (1) subwavelength silicon nanostructures can act as AR coating in the visible range due to the graded refractive index effect, (2) the GaN nanocolumns can effectively decrease the reflection losses over a broad wavelength range, and (3) the PL intensity is improved since the silicon absorption is eliminated and a strong blue emission is observed from the bottom side. This work also opens up promising opportunities for producing novel subwavelength AR coating in the visible range as well as GaN-Si hybrid devices using GaN-on-Si technology.

## Acknowledgements